Light-Controlled Reversible Release and Uptake of Potassium Ions from Ion-Exchanging Nanospheres

ARTICLE *in* ACS APPLIED MATERIALS & INTERFACES · JANUARY 2014

Impact Factor: 6.72 · DOI: 10.1021/am4049805 · Source: PubMed

2 AUTHORS:

Xiaojiang Xie
University of Geneva
32 PUBLICATIONS **274** CITATIONS

SEE PROFILE

Eric Bakker
University of Geneva
291 PUBLICATIONS **13,763** CITATIONS

SEE PROFILE

ACS APPLIED MATERIALS & INTERFACES

Research Article

www.acsami.org

Light-Controlled Reversible Release and Uptake of Potassium Ions from Ion-Exchanging Nanospheres

Xiaojiang Xie* and Eric Bakker*

Department of Inorganic and Analytical Chemistry, University of Geneva, Quai Ernest-Ansermet 30, CH-1211 Geneva, Switzerland

Supporting Information

ABSTRACT: Here, we report for the first time on photoswitchable nanospheres containing spiropyran (Sp) for reversible release and uptake of metal ions. K^+ is used as a model ion to demonstrate the chemical principle of this approach. Valinomycin is incorporated in the nanospheres to stabilize K^+. Upon UV illumination, Sp transforms to the more basic ring-opened merocyanine form, which takes up H^+ from the surrounding aqueous solution and expels K^+ from the nanospheres. The process can be reversed by irradiation with visible light to reduce the surrounding K^+ concentration.

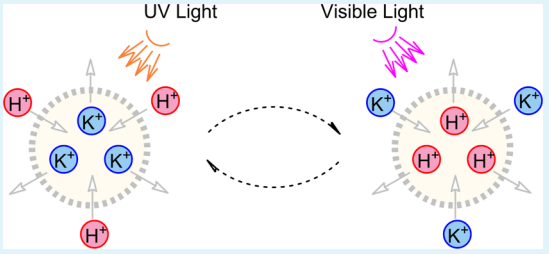

KEYWORDS: *photoswitching, potassium release, nanosphere, spiropyran, ion-selective*

INTRODUCTION

It has been recognized that metal ions such as Ca^{2+}, K^+, Zn^{2+}, and Mg^{2+} are involved in many vital biological processes.[1−6] Artificial control of parameters such as the concentration of certain ions or molecules can help to understand the function and mechanism of diverse in vivo biochemical processes.[7−9] It is challenging, however, to bring about ionic perturbation in a confined area without perturbation to other "innocent" areas. Such localized perturbation may allow one not only to observe cellular processes passively but also to stimulate cellular chemistry.

Phototriggered ionic perturbation is an attractive direction given by the relative ease of combining spatial and temporal control of the trigger by using readily available imaging equipment such as microscopes or spectrometers. Local increase of free Ca^{2+} concentration using caged calcium, such as NP-EGTA shown in Figure 1a, has been successful.[7,10−13] The photolysis, albeit irreversible, is able to raise the free Ca^{2+} level in a short time. Caged compounds for other chemical messengers such as ATP and glutamate have been also reported.[8,14] Photoacid generators (PAG) have been used to induce a pH imbalance in cancer cells.[15] Despite the continuing emergence of caging compounds for various targets in recent years, the number of ions that can be released is still rather limited.

The transformation of spiropyrans into protonated merocyanines in the presence of acid and the visible-light-induced release of protons from the latter species has been well-established.[16−19] UV light can also induce the spiropyran ring-opening reaction, and because the thermal back reaction is much slower than the ring-opening reaction,[20] the photostationary state is dominated by the merocyanines. Our group recently reported on the photoinduced basicity change of a derivative of the photochromic dye spiropyran in plasticized PVC membranes.[21] Protons can be taken up or released by the membrane because of a basicity change of Sp.[22] On the basis of light-induced ion-exchange or coextraction processes, active sensors for Cl^-, Na^+, and Ca^{2+} have been subsequently demonstrated.[23,24] We hypothesize that such light-induced ion-exchange and coextraction processes can be used to trigger local ion concentration perturbations as well. With readily available and highly selective ionophores for various ions, this may potentially form a new platform for light-induced ion perturbation.

In this work, we present a general approach to the realization of nanospheres that can alter the surrounding ion concentration upon light irradiation. K^+ is used as a model ion to demonstrate the chemical principle. The nanospheres are very small, stable, and biocompatible and can release K^+ upon UV illumination. The release of K^+ from the nanospheres is reversible. Upon visible-light irradiation, the nanospheres can take up K^+ and thus decrease the surrounding K^+ concentration. Direct monitoring of the ion concentration changes in solution phase is demonstrated with a K^+-selective probe.

EXPERIMENTAL SECTION

Reagents. Pluronic F-127 (F127), bis(2-ethylhexyl) sebacate (DOS), valinomycin (L), acetic acid, tetrahydrofuran (THF), potassium or sodium tetrakis-[3,5-bis(trifluoromethyl)phenyl]borate (K^+R^- or Na^+R^-), and poly(vinyl chloride) (PVC) were obtained from Sigma-Aldrich. Sp was synthesized according to the literature.[23,25] All solvents and reagents used were analytically pure unless otherwise specified. Aqueous solutions were prepared by dissolving the appropriate salts in Milli-Q-purified water.

Nanosphere Preparation. For spectroscopic experiments, 2.74 mg of NaTFPB, 1 mg of Sp, 8 mg of DOS, 25 mg of Pluronic F-127, and 4.1 mg of potassium ionophore valinomycin were dissolved in 3

Received: November 18, 2013
Accepted: January 29, 2014
Published: January 29, 2014

   dx.doi.org/10.1021/am4049805 | ACS Appl. Mater. Interfaces 2014, 6, 2666−2670

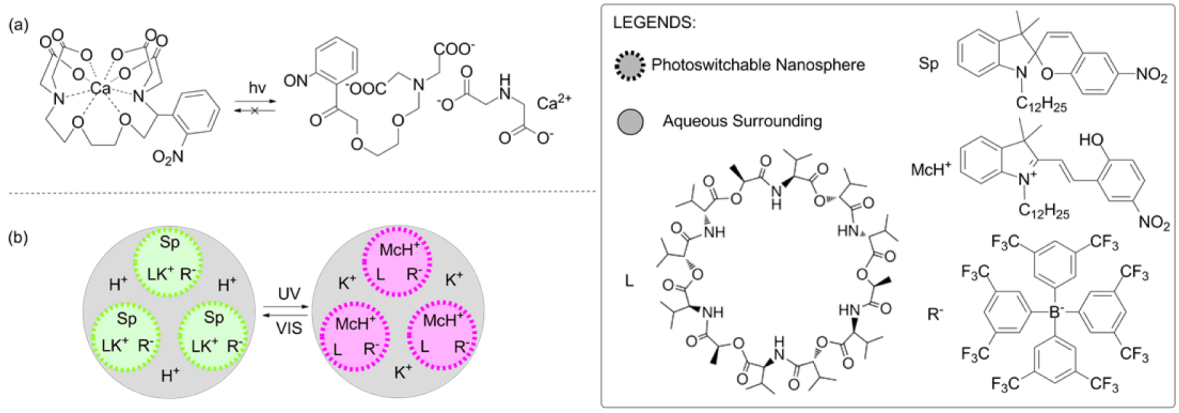

Figure 1. (a) Photolysis of caged calcium NP-EGTA. (b) Representation of light-controlled K^+ release and uptake with the photoswitchable nanospheres containing spiropyran.

mL of THF to form a homogeneous solution. The solution (0.5 mL) was pipetted and injected into 4.5 mL of deionized water on a vortex with a spinning speed of 1000 r/min. Compressed air was blown on the surface of the clear particle suspension for 20 min to remove THF. For Figure 3, a THF cocktail containing 2.66 mg of NaTFPB, 4.1 mg of valinomycin, and 3 mg of Sp were used for nanosphere preparation.

K^+-Selective Electrode. The membrane cocktail was prepared by dissolving 0.3 mg of KTFPB, 1.18 mg of valinomycin, 40 mg of PVC, and 80 mg of DOS in 1.5 mL of THF. The cocktail solution was then poured into a glass ring (22 mm in diameter) placed on a glass slide and dried overnight at room temperature under a dust-free environment. Small disks were punched from the cast films and mounted in Ostec electrode bodies (Ostec, Sargans, Switzerland).

Instrumentation and Measurement. The size of the nanospheres was measured with a Zetasizer Nano ZS (Malvern Inc.) particle-size analyzer. For transmission electron microscopy (TEM) imaging of the nanospheres, the nanosphere suspension was dispersed on to a Formvar/carbon film-coated TEM grid, counter-stained with uranyl acetate, dried in air, and visualized using a FEI Tecnai G2 Sphera transmission electron microscope.

The absorbance was measured with a UV−vis spectrometer (SPECORD 250 plus, Analytic Jena, AG, Germany). The fluorescence was measured with a fluorescence spectrometer (Fluorolog3, Horiba Jobin Yvon), with excitation at 365 nm (1 nm slit) or 409 nm (1 nm slit). Emission intensity at 650 nm (10 nm slit) was recorded for samples containing various K^+ concentrations in 10 mM acetic acid. The percentage of Mc, $[Mc]/[Sp_{tot}]$, was calculated using the following equation

$$[Mc]/[Sp_{tot}] = \frac{I}{I_{max} - I_{min}}$$

where I_{min} is the minimum emission intensity measured in blank and I_{max} is the maximum emission intensity measured in 1 mM KOH.

For direct monitoring of K^+ concentration as shown in Figure 3, the above-mentioned K^+ electrode was inserted into a glass cylinder together with a Ag/AgCl wire as the reference element (Figure S2). A Lambda DG-4 Plus xenon source (Sutter Instruments) was as light source for illumination with UV light (ZET365/20× filter, Chroma Inc.) and visible light (FF02-409/LP BrightLine long-pass filter, Semrock Inc.). On the bottom of the cylinder was placed a thin layer of nanosphere suspension (1 mM HCl and 10^{-5} M KCl). The EMF response from the K^+-selective electrode was recorded with an EMF-16 precision electrochemistry EMF interface from Lawson Laboratories Inc.

RESULTS AND DISCUSSION

Recently, we found that ultrasmall nanospheres (<100 nm in diameter) can be easily prepared by precipitation of bis(2-ethylhexyl) sebacate (DOS) and an amphoteric copolymer (Pluronic F-127) in water.[26] Lipophilic compounds could be incorporated in the nanoparticle core. Pluronic F-127 has been shown to exhibit attractive biocompatibility.[27] Including PVC in the nanosphere was found to result in a larger, less desired particle size. The nanospheres are very stable in solution and can be stocked over months without sedimentation. To develop nanospheres for localized ion perturbation, a photoswitchable compound, spiropyran (Sp), an ion-exchanger (R^-), and a K^+ ionophore valinomycin (L) were incorporated into the nanosphere core. Sp undergoes a UV-light-induced photoreaction to form a ring-opened merocyanine form (Mc) with a quantum yield of ca. 0.1.[28] The Mc form carries a phenolate group and exhibits much higher basicity than Sp.[23,24] As shown in Figure 1b, in the presence of H^+, the Mc form will be protonated to become positively charged McH^+. However, to protonate Mc, K^+, which was bound to L, must be ejected to keep the nanosphere core neutral (even in such small dimensions).[29] When illuminated with visible light (>409 nm), the McH^+ will transform back to Sp and release H^+, which will exchange with K^+ for charge-balance reasons, thereby reducing the surrounding K^+ concentration. This reverse process is difficult for caged compounds because photolysis reactions are normally irreversible. To our knowledge, a nanoscale tool that is able to both increase and reduce local ion concentration by light has never been reported before.

The size of the nanospheres was determined by dynamic light scattering (DLS) as well as transmission electron microscopy (TEM) (see Figure S1 in the Supporting Information). An average diameter of 71 nm was obtained from DLS with a polydispersity index of 0.23, indicating a relatively narrow size distribution. The size obtained from light-scattering measurements is slightly larger than that observed in TEM. Although the former technique is dependent on hydrodynamic size,[26] shrinkage and aggregation of the nanospheres were observed in TEM, and outgassing of the plasticizer more likely explains the size difference.

Because the release and uptake of K^+ is accompanied with protonation of Mc and deprotonation of McH^+, the processes can be observed spectroscopically, as both Mc and McH^+ are fluorescent. However, the emission intensity at 650 nm for Mc is much higher than for McH^+. As shown in Figure 2a, upon UV (365 nm) illumination, the fluorescence intensity increases because of the ring-opening photoreaction of Sp. In the absence of K^+, the photoproduct is protonated to form McH^+, for which the emission intensity is relatively low. As the K^+ concentration

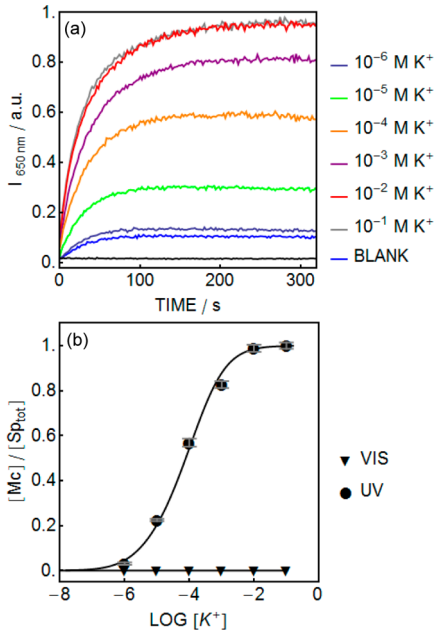

Figure 2. (a) Fluorescence emission intensity (650 nm) of the nanospheres with various KCl concentrations as indicated and 10 mM acetic acid as buffer. The black line was recorded with visible light (409 nm) as excitation, and the others were excited with 365 nm UV light. (b) Percentage of Mc ([Mc]/[Sp_{tot}]) under UV and visible-light irradiation from panel a. Error bars are standard deviations.

increases, more Mc is formed, and the percentage of McH^+ is reduced because of the exchange between K^+ and H^+. Therefore, the steady-state emission intensity increases with increasing K^+ concentration, confirming the exchange between H^+ and K^+. Moreover, fitting the calibration with equilibrium response theory gives satisfactory results (Figure 2b), indicating that electroneutrality indeed holds for the nanosphere bulk. When irradiated with visible light (409 nm), the ring-opened forms are suppressed, which renders K^+ more competitive than H^+ because the basicity of Sp is very low.

Although spectroscopic characterization shows very encouraging results, it is only indirect evidence because the release and uptake of K^+ are inferred from the behavior of the protonation of the incorporated dye. To obtain direct evidence that K^+ in the aqueous surroundings is being perturbed by the nanospheres, a K^+-selective electrode was used to monitor the K^+ concentration in the aqueous solution containing the photoswitchable nanospheres. The setup is shown in Figure S2; a confined layer (ca. 1 mm) of suspension containing the nanospheres was pipetted into a transparent glass cylinder. A K^+-selective electrode (for the preparation procedure, see the Experimental Section) was placed in direct contact with the suspension, and light illumination was brought about from the bottom of the cylinder. The K^+ concentration was obtained by comparing the electromotive force (EMF) readout with an external calibration curve (see Figure S3 in the Supporting Information).

As shown in Figure 3, when UV light (ca. 2.9 mW cm^{-2}) was switched on, a substantial potential jump of ca. 78 mV that corresponds to a ca. 25-fold K^+ concentration increase was achieved after 30 s of illumination. Upon illumination with visible light, the K^+ concentration dropped by a factor of 17, indicating K^+ uptake into the nanospheres. Compared to a caged compound with a milliseconds response time, the current

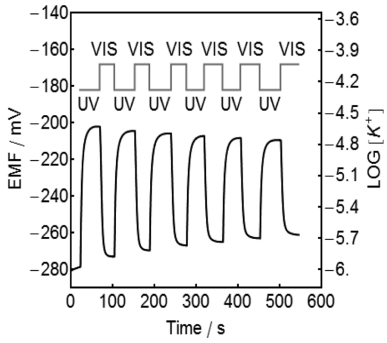

Figure 3. Direct monitoring of K^+ concentration oscillation (lower trace) induced by the photoswitchable nanospheres in 1 mM HCl under alternating UV and visible-light illumination using a K^+-selective probe. The applied light sequence is indicated by the gray square wave at the top.

system is appreciably slower. The kinetics are limited by the photoreaction rate of Sp, which, in this case, is rather sluggish because of the relatively weak light intensity. The conversion from excited-state Sp to Mc form has been shown to take place in less than 10 ps,[30,31] and the overall conversion from Sp to Mc is proportional to light intensity. With typical laser intensities (ca. 100 mW cm^{-2}) from a conventional confocal fluorescence microscope, the response time should approach tens of microseconds.

The light-triggered K^+ perturbation was observed under acidic conditions because of the relatively low basicity of the ring-opened Mc in the nanospheres. The pK_a of the Mc form was determined to be ca. 4.6 in the nanospheres by comparison of similar particles with chromoionophore I, which has a pK_a of ca. 11.4 in PVC-DOS membrane[32] and ca. 7.4 in the nanospheres. For applications at physiological pH, the basicity needs be increased, which could potentially be achieved through structural modification of the spiropyran or by improving on the nanosphere core materials

Some deterioration in the repeatability was noted with time. This is probably due to photofatigue of Sp,[23,30,33,34] as stronger light resulted in even larger attenuation of the signal (see Figure S4 in the Supporting Information). A similar effect was also observed in spectroscopic characterization (see Figure S5 in the Supporting Information). The choice of light intensity should be a balance between the required speed and photostability.

Although the photolysis of conventional caged ions (Figure 1a) is irreversible, the ion concentration after light activation is normally thermally independent. The back reaction of spiropyran from the ring-opened form to the ring-closed form can be accelerated by light, but it is also thermally driven.[30] Therefore, it is necessary to confirm that the UV-induced K^+ concentration increase remains indifferent when illumination is stopped. If the thermal back reaction were too rapid, then the UV-induced elevated K^+ concentration should start to decrease. However, after UV-light illumination, the EMF response from the K^+ selective electrode was found to remain stable in the dark (see Figure S6 in the Supporting Information), which confirms that the thermal back reaction for McH^+ is in fact sufficiently slow.

Spiropyran has recently been reported to decompose under acidic aqueous conditions,[16] prompting us to study its thermal stability. As shown in Figure S7, when the nanospheres were stored in 1 mM HCl, Sp gradually protonated to form MCH^+, resulting in an increase in the absorbance around 420 nm.

dx.doi.org/10.1021/am4049805 | ACS Appl. Mater. Interfaces 2014, 6, 2666−2670

However, this was not the case in the presence of K^+ in the nanosphere suspension. As shown in Figure S8, the absorption spectra remained the same even after 20 h in the dark without the appearance of the absorption maxima from Mc or McH^+ unless UV light was used to activate the nanospheres. No dramatic change in the absorption spectra after UV-light illumination was observed, indicating that the nanospheres are thermally quite stable.

Selectivity is also an important aspect one should consider in designing any molecular probe or caging reagent. Ensuring selectivity is usually challenging in developing caged reagents. However, for the system we present here, the selectivity may be superior because of the availability of very selective ionophores.[35] For this model system, valinomycin, for which the selectivity to K^+ is known to be excellent, was chosen as the K^+ receptor.[36,37] The selectivity was confirmed with fluorescence spectroscopy. As shown in Figure 4, other metal ions such as Na^+, Mg^{2+}, and Ca^{2+} did not cause appreciable interference.

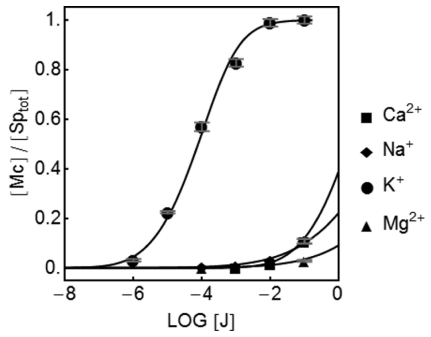

Figure 4. Selectivity of the photoswithable nanospheres for K^+ determined in 10 mM acetic acid in fluorescence mode.

CONCLUSIONS

A general approach to develop nanospheres that can bring about localized ion concentration perturbation by light has been presented with K^+ as a model ion. The nanospheres can be conveniently produced by precipitation in large quantities. The photoswitchable compound Sp was incorporated into the nanospheres. Upon UV irradiation, the nanospheres increased the surrounding K^+ concentration by releasing K^+. Unlike most caged reagents, the process could be reversed by illumination with visible light, thereby resulting in a subsequent decrease in the surrounding K^+ concentration. The nanospheres exhibited excellent selectivity for K^+ and may form the chemical basis for a new generation of cagelike nanomaterials.

ASSOCIATED CONTENT

Supporting Information

Transmission electron microscopic image of the photoswitchable nanospheres, schematic representation for the setup used to direct monitoring light triggered K^+ level oscillation in a suspension of photoswitchable nanospheres, external calibration in 1 mM HCl for the K^+-selective potentiometric probe, K^+ concentration oscillation induced by the photoswitchable nanospheres in 1 mM HCl under UV and visible-light illumination, photofatigue effect from the nanospheres under spectroscopic interrogation, EMF response from the K^+-selective probe recorded when the nanospheres were first illuminated by UV and kept in the dark for 20 s before visible light was switched on, absorption spectra obtained every 0.5 h for photoswitchable nanospheres in 1 mM HCl in the dark, and absorption spectra of photoswitchable nanospheres in 10 mM acetic acid containing 1 mM KCl. This material is available free of charge via the Internet at http://pubs.acs.org.

AUTHOR INFORMATION

Corresponding Authors

*E-mail: xiaojiang.xie@unige.ch.
*E-mail: eric.bakker@unige.ch.

Notes

The authors declare no competing financial interest.

ACKNOWLEDGMENTS

We thank the Swiss National Science Foundation (SNF) for financial support. We thank Dawid Kedracki and Istvan Szilágyi for help with the light-scattering experiments and Christoph Bauer for performing the TEM imaging.

REFERENCES

(1) Wang, K.; Terrenoire, C.; Sampson, K. J.; Iyer, V.; Osteen, J. D.; Lu, J.; Keller, G.; Kotton, D. N.; Kass, R. S. Biophysical Properties of Slow Potassium Channels in Human Embryonic Stem Cell Derived Cardiomyocytes Implicate Subunit Stoichiometry. *J. Physiol.* **2011**, *589*, 6093−6104.

(2) Minami, A.; Sakurada, N.; Fuke, S.; Kikuchi, K.; Nagano, T.; Oku, N.; Takeda, A. Inhibition of Presynaptic Activity by Zinc Released from Mossy Fiber Terminals during Tetanic Stimulation. *J. Neurosci. Res.* **2006**, *83*, 167−176.

(3) Dudek, F. E. Zinc and Epileptogenesis. *Epilepsy Curr.* **2001**, *1*, 66.

(4) Lipscomb, W. N.; Sträter, N. Recent Advances in Zinc Enzymology. *Chem. Rev.* **1996**, *96*, 2375−2434.

(5) Kass, R. S.; Freeman, L. C. Potassium Channels in the Heart: Cellular, Molecular, and Clinical Implications. *Trends Cardiovasc. Med.* **1993**, *3*, 149−159.

(6) Michel, H.; Oesterhelt, D. Electrochemical Proton Gradient across the Cell Membrane of Halobacterium Halobium: Effect of N,N′-Dicyclohexylcarbodiimide, Relation to Intracellular Adenosine Triphosphate, Adenosine Diphosphate, and Phosphate Concentration, and Influence of the Potassium Gradient. *Biochemistry* **1980**, *19*, 4607−4614.

(7) Ellis-Davies, G. C. R. Neurobiology with Caged Calcium. *Chem. Rev.* **2008**, *108*, 1603−1613.

(8) Yu, H.; Li, J.; Wu, D.; Qiu, Z.; Zhang, Y. Chemistry and Biological Applications of Photo-Labile Organic Molecules. *Chem. Soc. Rev.* **2010**, *39*, 464−473.

(9) Figueroa, L.; Shkryl, V. M.; Zhou, J.; Manno, C.; Momotake, A.; Brum, G.; Blatter, L. A.; Ellis-Davies, G. C. R.; Ríos, E. Synthetic Localized Calcium Transients Directly Probe Signalling Mechanisms in Skeletal Muscle. *J. Physiol.* **2012**, *590*, 1389−1411.

(10) Adam, S. R.; Kao, J. P. Y.; Grynkiewicz, G.; Minta, A.; Tsien, R. Y. Biologically Useful Chelators That Release Ca^{2+} upon Illumination. *J. Am. Chem. Soc.* **1988**, *110*, 3212−3220.

(11) Ellis-Davies, G. C. R.; Kaplan, J. H. A New Class of Photolabile Chelators for the Rapid Release of Divalent Cations: Generation of Caged Calcium and Caged Magnesium. *J. Org. Chem.* **1988**, *53*, 1966−1969.

(12) Adams, S. R.; Kao, J. P. Y.; Tsien, R. Y. Biologically Useful Chelators that Take up Calcium(2+) upon Illumination. *J. Am. Chem. Soc.* **1989**, *111*, 7957−7968.

(13) Ellis-Davies, G. C. R.; Kaplan, J. H. Nitrophenyl-EGTA, a Photolabile Chelator that Selectively Binds Ca^{2+} with High Affinity and Releases It Rapidly upon Photolysis. *Proc. Natl. Acad. Sci. U.S.A.* **1994**, *91*, 187−191.

(14) Olson, J. P.; Kwon, H.-B.; Takasaki, K. T.; Chiu, C. Q.; Higley, M. J.; Sabatini, B. L.; Ellis-Davies, G. C. R. Optically Selective Two-

Photon Uncaging of Glutamate at 900 nm. *J. Am. Chem. Soc.* **2013**, *135*, 5954−5957.
(15) Yue, X.; Yanez, C. O.; Yao, S.; Belfield, K. D. Selective Cell Death by Photochemically Induced pH Imbalance in Cancer Cells. *J. Am. Chem. Soc.* **2013**, *135*, 2112−2115.
(16) Hammarson, M.; Nilsson, J. R.; Li, S.; Beke-Somfai, T.; Andréasson, J. Characterization of the Thermal and Photoinduced Reactions of Photochromic Spiropyrans in Aqueous Solution. *J. Phys. Chem. B* **2013**, *117*, 13561−13571.
(17) Kong, L.; Wong, H.-L.; Tam, A. Y.-Y.; Lam, W. H.; Wu, L.; Yam, V. W.-W. Synthesis, Characterization, and Photophysical Properties of Bodipy-Spirooxazine and -Spiropyran Conjugates: Modulation of Fluorescence Resonance Energy Transfer Behavior via Acidochromic and Photochromic Switching *ACS Appl. Mater. Interfaces* [Online early access]. DOI: 10.1021/am404242a. Published Online: Jan 17, **2014**.
(18) Ziółkowski, B.; Florea, L.; Theobald, J.; Benito-Lopez, F.; Diamond, D. Self-Protonating Spiropyran-co-NIPAM-co-Acrylic Acid Hydrogel Photoactuators. *Soft Matter* **2013**, *9*, 8754−8760.
(19) Giordani, S.; Cejas, M. A.; Raymo, F. M. Photoinduced Proton Exchange between Molecular Switches. *Tetrahedron* **2004**, *60*, 10973−10981.
(20) Levitus, M.; Talhavini, M.; Negri, R. M.; Atvars, T. D. Z.; Aramendía, P. F. Novel Kinetic Model in Amorphous Polymers. Spiropyran-Merocyanine System Revisited. *J. Phys. Chem. B* **1997**, *101*, 7680−7686.
(21) Mistlberger, G.; Crespo, G. A.; Xie, X.; Bakker, E. Photodynamic Ion Sensor systems with Spiropyran: Photoactivated Acidity Changes in Plasticized Poly(vinyl chloride). *Chem. Commun.* **2012**, *48*, 5662−5664.
(22) Xie, X.; Crespo, G. A.; Mistlberger, G.; Bakker, E. Photocurrent Generation Based on a Light-Driven Proton Pump in an Artificial Liquid Membrane *Nat. Chem.* [Online early access]. DOI: 10.1038/nchem.1858. Published Online: Feb 2, **2014**.
(23) Xie, X.; Mistlberger, G.; Bakker, E. Reversible Photodynamic Chloride-Selective Sensor based on Photochromic Spiropyran. *J. Am. Chem. Soc.* **2012**, *134*, 16929−16932.
(24) Mistlberger, G.; Xie, X.; Pawlak, M.; Crespo, G. A.; Bakker, E. Photoresponsive Ion Extraction/Release Systems: Dynamic Ion Optodes for Calcium and Sodium Based on Photochromic Spiropyran. *Anal. Chem.* **2013**, *85*, 2983−2990.
(25) Renkecz, T.; Mistlberger, G.; Pawlak, M.; Horváth, V.; Bakker, E. Molecularly Imprinted Polymer Microspheres Containing Photoswitchable Spiropyran-Based Binding Sites. *ACS Appl. Mater. Interfaces* **2013**, *5*, 8537−8545.
(26) Xie, X.; Mistlberger, G.; Bakker, E. Ultrasmall Fluorescent Ion-Exchanging Nanospheres Containing Selective Ionophores. *Anal. Chem.* **2013**, *85*, 9932−9938.
(27) Wang, X.-d.; Stolwijk, J. A.; Lang, T.; Sperber, M.; Meier, R. J.; Wegener, J.; Wolfbeis, O. S. Ultra-Small, Highly Stable, and Sensitive Dual Nanosensors for Imaging Intracellular Oxygen and pH in Cytosol. *J. Am. Chem. Soc.* **2012**, *134*, 17011−17014.
(28) Görner, H. Photochromism of Nitrospiropyrans: Effects of Structure, Solvent and Temperature. *Phys. Chem. Chem. Phys.* **2001**, *3*, 416−423.
(29) Bakker, E.; Bühlmann, P.; Pretsch, E. Carrier-Based Ion-Selective Electrodes and Bulk Optodes. 1. General Characteristics. *Chem. Rev.* **1997**, *97*, 3083−3132.
(30) Minkin, V. I. Photo-, Thermo-, Solvato-, and Electrochromic Spiroheterocyclic Compounds. *Chem. Rev.* **2004**, *104*, 2751−2776.
(31) Krysanov, S. A.; Alfimov, M. V. Ultrafast Formation of Transients in Spiropyran Photochromism. *Chem. Phys. Lett.* **1982**, *91*, 77.
(32) Qin, Y.; Bakker, E. Quantitive Binding Constants of H^+-Selective Chromoionophores and Anion Ionophores in Solvent Polymeric Sensing Membranes. *Talanta* **2002**, *58*, 909−918.
(33) Wen, G.; Yan, J.; Zhou, Y.; Zhang, D.; Mao, L.; Zhu, D. Photomodulation of the Electrode Potential of a Photochromic Spiropyran-Modified Au Electrode in the Presence of Zn^{2+}: A New Molecular Switch Based on the Electronic Transduction of the Optical Signals. *Chem. Commun.* **2006**, 3016−3018.
(34) Tong, R.; Hemmati, H. D.; Langer, R.; Kohane, D. S. Photoswitchable Nanoparticles for Triggered Tissue Penetration and Drug Delivery. *J. Am. Chem. Soc.* **2012**, *134*, 8848−8855.
(35) Bühlmann, P.; Pretsch, E.; Bakker, E. Carrier-Based Ion-Selective Electrodes and Bulk Optodes. 2. Ionophores for Potentiometric and Optical Sensors. *Chem. Rev.* **1998**, *98*, 1593−1687.
(36) Anker, P.; Jenny, H. B.; Wuthier, U.; Asper, R.; Ammann, D.; Simon, W. Determination of Potassium Ion Concentration in Blood Serum with a Valinomycin-Based Silicone Rubber Membrane of Universal Applicability to Body Fluids. *Clin. Chem.* **1983**, *29*, 1447−1448.
(37) Pietrzak, M.; Meyerhoff, M. E. Determination of Potassium in Red Blood Cells Using Unmeasured Volumes of Whole Blood and Combined Sodium/Potassium-Selective Membrane Electrode Measurements. *Anal. Chem.* **2009**, *81*, 5961−5965.